HHS Public Access

Author manuscript

IEEE Trans Inf Technol Biomed. Author manuscript; available in PMC 2015 October 14.

Published in final edited form as:

IEEE Trans Inf Technol Biomed. 2012 November ; 16(6): 1208–1215. doi:10.1109/TITB.2012.2207399.

Implantable Ultralow Pulmonary Pressure Monitoring System for Fetal Surgery

Mozziyar Etemadi [Student Member, IEEE],
Department of Bioengineering and Therapeutic Sciences, the UC Berkeley and UCSF Joint Graduate Group in Bioengineering, and the Division of Pediatric Surgery, University of California, San Francisco, CA 94720 USA (Mozziyar.Etemadi@ucsf.edu).

J. Alex Heller [Student Member, IEEE],
Department of Bioengineering and Therapeutic Sciences, University of California, San Francisco, CA 94720 USA (James.Heller@ucsf.edu).

Samuel C. Schecter,
Division of Pediatric Surgery, University of California, San Francisco, CA 94720 USA (Samuel.Schecter@ucsfmedctr.org).

Eveline H. Shue,
Division of Pediatric Surgery, University of California, San Francisco, CA 94720 USA (Eveline.Shue@ucsfmedctr.org).

Doug Miniati, and
Division of Pediatric Surgery, University of California, San Francisco, CA 94720 USA (Douglas.Miniati@ucsfmedctr.org).

Shuvo Roy [Member, IEEE]
Department of Bioengineering and Therapeutic Sciences, University of California, San Francisco, CA 94720 USA (Shuvo.Roy@ucsf.edu).

Abstract

Congenital pulmonary hypoplasia is a devastating condition affecting fetal and newborn pulmonary physiology, resulting in great morbidity and mortality. The fetal lung develops in a fluid-filled environment. In this paper, we describe a novel, implantable pressure sensing and recording device which we use to study the pressures present in the fetal pulmonary tree throughout gestation. The system achieves 0.18 cm H_2O resolution and can record for 21 days continuously at 256 Hz. Sample tracings of *in vivo* fetal lamb recordings are shown.

Keywords

Data logger; fetal surgery; ultralow pressure sensing

I. Introduction

Congenital pulmonary hypoplasia is a devastating condition arising from a variety of fetal and maternal conditions such as oligohydramnios, chylothorax, intrathoracic mass effect, and preterm labor [1]. Whatever the cause, the resulting newborn lung is unable to exchange

gas between the atmosphere and the bloodstream, and despite advances in engineering and medicine, pulmonary hypoplasia continues to maintain high rates of morbidity and mortality [1], [2].

Although there are many genetic, biochemical, and physiologic factors studied in relation to this disease, most center around the concept that mechanical forces present in the lung during gestation contribute to the healthy or diseased development of lung tissue [1]. The mechanical environment of the fetal lung is very different from that of a newborn, yet it is the fetal lung environment which uniquely determines whether the lung will function immediately after birth. In essence, the fetus has nine months of “preparation time” in which the lung is in a fluid-filled environment after which it must immediately expel the fluid and breathe oxygen-rich air.

In the fetal environment, the lung is filled with fluid as well as surrounded by it, rendering hydrostatic pressures across the lung tissue close to zero. In contrast, a water-logged lung outside the amniotic sac is weighed down by the water within it, leading to respiratory distress and tissue damage. In the fetal environment, the lungs themselves are producing the majority of the liquid inside of them, and thus, they are able to control their own volume and stretch [3]. This is enhanced by simultaneous control of the glottic muscles, which contract to trap fluid inside the lung and further “stretch open” the lung with trapped fluid [4]. In the newborn, only the diaphragm can control lung volume, requiring a delicate pressure balance between lung, pleural space, and thoracic cavity.

The diaphragm itself has been predicted to play a role in fetal development as well. Epochs of diaphragmatic contraction coincident with glottic closure are referred to as “fetal breathing” [3], [5]. There are two types of contractions that have been generally observed: small contractions unable to move fluid in and out of the lungs, and larger contractions resulting in a large influx and efflux (gasps) of fluid, creating wide pressure swings in the trachea and lungs [6].

A. Recording Fetal Breathing

Unfortunately, attempts to classify fetal diaphragmatic activity—and the resultant pressures in the pulmonary tree—were largely abandoned when transducers and circuitry had not yet reached the level of accuracy, power efficiency, and biocompatibility that we have today. Also, the invasiveness of such methods typically limits their use to animal models such as the fetal lamb. Much of the earlier work relied on externalized transducers referred to atmosphere, that is, catheters exiting the lamb fetus, through the uterine wall, through the abdominal wall of the ewe, out into the open. In addition to causing surgical complications, these techniques fundamentally do not use closed fluid systems and thus may not fully represent the true pressures present in the pulmonary tree. These systems could not be used for more than a few days and were unable to capture developmental changes in pulmonary physiology occurring over weeks. Early [7] and recent [8] feasibility studies in fetal telemetry rely on bulky, costly systems consisting of antennae, power supplies, and computers nearby the animal. These systems, if further engineered beyond the feasibility stage, could likely be useful in our application because they remove the largest component of the implant (the battery). However, the one commercially available telemetry system

(from Data Sciences International) is still relatively range limited and very costly, making it infeasible for long-term studies of many animals.

Significant advances have been made in non-fetal, implanted physiologic monitors. The Medtronic Chronicle pacemaker includes a pressure sensor at its tip and data storage and inductive data transfer in its can [9]. This device, in addition to being proprietary and costly, has too wide of a dynamic range and not fine enough resolution for fetal use. Our group demonstrated a passive, implanted *LC*-tank circuit consisting of a microelectromechanical system inductor and pressure sensitive capacitor [10]. Pressure changes on the capacitor lead to changes in resonance frequency which are picked up by an external "grid-dip" style detector. While allowing for wireless, batteryless operation, the external device is relatively complex, bulky, and costly (many groups use a benchtop network analyzer). Furthermore, the coupling efficiency (and thus observed quality factor) of such an inductive link is strongly dependent on tissue thickness, eddy currents, and other factors which limit the final sensitivity of such a system. Low-power, high-accuracy, implantable systems have been demonstrated, but their power savings is due to a low (Sub-Hertz) sampling rate [11]. While existing systems work fairly well for their intended applications, none of them are appropriate for the duration, sampling rate, and sensitivity we require.

Although scarce, previously presented pressure data suggest one basic fact: slow, sustained ultralow frequency (ULF) pressure changes must relate to the slow buildup of fluid from the lung tissue against a closed glottis, and faster, dynamic (1–20 Hz) pressure changes must have to do with diaphragmatic muscle contraction. These pressures, both the ULF and dynamic components, are being sensed by the lung tissue as strain. There is no evidence to suggest that tissue cannot respond to both fast and slow strain changes. Taking a fresh approach, in this study, we design, build, and test a fully implantable pressure data logger with high dynamic range and bandwidth, with the goal of measuring the true pressures in the pulmonary tree throughout gestation. With these pressures characterized, we may be able to better effect pulmonary growth with *in utero* devices or altered neonatal ventilatory strategies.

II. Design, Fabrication, and Testing

A. Design Constraints and Parameters

To capture both the slowly varying ULF pressure due to glottic activity, and dynamic diaphragmatic contractions, we require a system with a wide dynamic range and frequency response, as well as relatively high resolution. Based on the previous literature detailed above, *we would like to achieve ±20 cm H_2O range with at least 1 cm H_2O resolution, at 20 Hz bandwidth*. The system must also be able to be surgically implanted in at least two fetal lambs simultaneously for 21 days and record continuously throughout this time. The system must have minimal impact in the fetus and ewe—allowing for as close as possible to normal gestation to occur.

B. Design Overview

Briefly, the measurement system consists of four pressure sensors, analog amplification and filtering, data acquisition, and microcontroller-based data storage on a microSD card. Each

sensor, two per fetus, is affixed to the skin near the measurement site and a 2-ft-long cable traverses the uterus to the abdominal cavity. Here, the cable connects to a titanium enclosure containing the data logging circuitry and battery. The enclosure is thus implanted in the maternal abdomen and the sensors in the uterus. This is outlined in Fig. 1 and details follow in the sections below.

C. Electronics Design

1) Pressure Sensor Selection—The principle requirement of our pressure sensor is for it to measure a differential fluid pressure—that is, pressure between the trachea or oropharynx and the amniotic cavity. Since the fetus does not "feel" atmospheric pressure directly and has no access to the outside air, a gauge sensor is not appropriate or practical. Another key requirement of the sensor is that it has the appropriate sensitivity and noise characteristics to measure the very small (on the order of a few centimeters of water) pressures of interest. Unfortunately, there are very few commercially available sensors that are both differential and fluid compatible (so-called wet–wet sensors), and at the time of writing this manuscript, there is only one that is also able to sense very small pressures and is small enough itself to be implanted. This is the Omega PX-26 (Omega Inc, Stamford, CT), differential +/− 1 PSI full scale model which is readily available for 40 U.S. dollars. Its specifications are listed in Table I.

This sensor has no internal amplification and instead provides the user with a current limited Wheatstone bridge that has an output proportional to the differential pressure. One PSI is equal to 1.67 mV per volt of excitation on the bridge. Because our excitation voltage is around 3.4 V, the maximum transducer sensitivity is 80.7 μV per cm H_2O. We are interested in pressures in the range of −20 to +20 cm of water, to capture both the gradual shifts in pressure due to glottic activity, as well as transient spikes due to the diaphragm. Our maximum possible acceptable resolution is 1 cm of water over this range, which corresponds to signal level of approximately 80 μV.

2) Analog Amplifier—Each pressure sensor has a dedicated amplification and filtering stage following the output of its Wheatstone bridge. Both the bridge and analog circuitry are shown in Fig. 2. Every attempt was made to obtain low noise—achieving high resolution, ultralow pressure readings—while also drawing little power. As such, the front end is a commercially available, low-noise precision instrumentation amplifier (Analog Devices, Norwood, MA) with a gain of 900. At the source impedance of the sensor, the voltage noise of the amplifier dominates at 0.6 μVpp (input referred), giving us a corresponding minimum signal-to-noise ratio (for the smallest possible signal) of 30 dB. Its reference is set precisely to mid-supply by a buffered, manually adjustable voltage divider fed from a low-noise operational amplifier (Linear Technologies, Milpitas, CA). Following the instrumentation amplifier is a fourth-order, 50 Hz cutoff (−3dB) Sallen–Key low-pass filter to reduce aliasing artifacts. Attenuation at Nyquist is approximately 44 dB.

3) Analog-to-Digital (A/D) Conversion—The A/D conversion is built into the Atmega 1284P microcontroller (Atmel Inc., Norway). Care was taken to ensure that analog and digital grounds and supplies were separated and only connected by one point. In addition, a

choke-bypass network connected the analog power to the battery, to eliminate ripples from the digital side from corrupting the analog signal. Furthermore, the analog supply was tied both to the input of the Wheatstone bridge as well as the reference pin of the A/D converter, ensuring a ratiometric output that is supply insensitive. This removed the need for a voltage regulator, thus allowing for lower noise, fewer components, and lower power draw and compensation for the gradual decline in battery voltage.

4) Microcontroller Firmware—The Atmega 1284P was chosen due to its low sleep current, large memory, and flexible timer and peripheral options. The sampling clock is driven by an asynchronous, 65.536 kHz crystal oscillator. When fed into an 8-bit counter, an overflow occurs precisely 256 times per second. This overflow triggers an interrupt, which wakes up the microcontroller. Because the microcontroller's “synchronous” clock is an internal *LC*-tank (8 MHz), it wakes up very quickly (less than ten cycles) and rapidly acquires all four channels of input.

Each sample was acquired at 8-bit resolution, and filled into a 2-MB memory buffer. Thus, two seconds of all four channels fills up the buffer. In general, our system's power consumption, code base, etc., is periodic with a period of two seconds. Eight samples before the buffer is filled (that is, at sample 505 of 512 for each channel), the process of buffer writing to SD card is begun. This is the cornerstone of achieving low power with a microSD card—an incorrectly initiated write statement can lead to seconds of “idle” SD card time which can use anywhere from 5-30 milliamps of current.

The reader should first note that an SD card accepts data in “pages” of 512 bytes. While waiting for a complete 512 bytes or any multiple, the card remains “idle” instead of asleep, using significantly more current. While it is being received, this “page” is stored in some form of temporary storage until it is actually written to the NAND flash, in a card-specific chunk size. For the card used in this study, this chunk size was 1024 bytes, or two pages.

Three aspects of the code contribute to the lowest power possible operation. First, while procedurally more simple, samples are *not* given to the card as they are retrieved from the A/D converter. Instead, they are stored in a memory buffer and written as fast as the 8-MHz clock rate of the microcontroller allows. Otherwise, because the page size for the SD card is 512 bytes, the card would “wait” until 512 bytes (512 samples) were received in order to go back to sleep—this would keep the card in “idle” mode (5–30 mA) between samples.

Second, it is crucial to send a “pre-erase” command to the SD card to inform it of the size of the incoming data. This informs the card of the incoming data size and allows for the card, after receiving the data, to write the data to NAND as efficiently as possible. Finally, one must release the chip select after the final byte is written, to allow the card to finish the write operation at its own, fast internal clock cycle. If this is not done, the microcontroller and SD card must remain awake and communicate until all data are written to NAND—a process that can take several samples.

Fig. 3 details our write operation. At all samples except 505–512, only the microcontroller awakes and takes a sample using its built in A/D, stores it to SRAM, then goes to sleep. This

process consumes < 10 mA for a very short time window. At sample 505, the microcontroller awakes, takes a sample, and then tells the microSD card to expect an incoming 2 MB of data. Following this, it sends the first 250 of 2048 samples in memory. At sample 506, another sample is taken, and 250–512 are sent, completing the first page. The process is repeated during samples 507 and 508, where 513–1024 are written. Upon the completion of the second page, the microSD card, now with a full 1024 chunk, initiates a write to NAND. The process during samples 505–508 is repeated for 509–512, and chip select is released. The microSD, having expected 2 MB, immediately finishes the write operation after chip select is released.

This write process allows for our entire system to maintain a relatively low (2.2 mA) average supply current, including all analog circuitry. As such, a 3-Ah lithium polymer battery was used as the main power supply, providing well over 21 days of battery life robust to battery aging and declines in capacity due to the pulsed nature of the microSD card's supply current. The reader should note that while microSD cards are not typically used or designed for synchronous, real-time applications, our technique allows for nearly deterministic power consumption. Finally, the information here was all synthesized from publicly available documents and websites—thus presenting an inexpensive, off-the-shelf, low pin-count, removable storage solution for data logging applications, free of licensing requirements typically present with flash memory chips.

D. Mechanical Design and Surgical Considerations

To achieve long implant time, minimal reaction, and be unobtrusive to the fetus, every attempt was made to use highly biocompatible materials and minimize size. The PX-26 sensors themselves, while compatible with fluid on their measurement ports, are not hermetically sealed. Furthermore, the sensor's Wheatstone bridge is only accessible through four exposed metal pins. These four pins were presoldered to a four-conductor, Kevlar reinforced audio cable. This cable was then sheathed in a silicone tube. The end nearest the sensor was tucked up as close as possible to the sensor, along with two more silicone tubes affixed to the measurement and reference port of the sensor. This three tube and sensor entity was put into a custom 3-D printed mold which was then filled with liquid silicone and allowed to cure for three days.

The resulting water-tight “mass” of silicone (see Fig. 4) has three interfaces: a reference tube, a measurement tube, and a tube with our four-conductor cable. The other end of the cable tube was fitted with a barb-to-NPT adapter, which was screwed directly into the titanium box. The wire itself was attached to the printed circuit board (PCB) with a Molex picoBlade connector once inside the box.

The titanium enclosure was milled using a computer numerical control (CNC) system out of one solid block of metal, with special care taken to ensure that all edges were rounded and no rough surfaces remained. Small holes were introduced into the corners of the box to allow for a suture needle to pass through, with the goal of easily and tightly attaching the enclosure to the abdominal wall, ensuring no bowel is impinged between box and muscle. The lid to the enclosure was similarly milled out of titanium, and affixed to the box with

titanium screws and a custom laser-cut silicone gasket. The assembled enclosure measures 3.8″ × 2″ × 1″.

E. Validation and Calibration

1) Pressure Calibration—To calibrate the system, pressure was applied simultaneously to our system and two gold standard sensors, both the GE Druck DPI 104. Since the DPI 104 sensors are gauge sensors, two were needed: one connected to the sense port of each of our sensors, and one to the reference port. The pressure was applied in a step-wise, increasing manner using a programmable syringe pump. Resultant pressures from the DPI 104s was recorded directly to PC, and later "lined up" to the pressures from our device. Each pressure was held for approximately 15 s, with the compared value chosen in the middle of this window, to ensure that slight variations in lining up the signals would not affect our calibration. A plot of actual pressure versus bit code was generated for each sensor, as well as a Bland–Altman curve, both in Fig. 5. Unfortunately, the DPI 104, while it specifies a maximum resolution of 0.1 cm H_2O, in practice exhibits many transient pressure fluctuations of 0.1–0.3 cm H_2O in magnitude, perhaps explaining the relatively large limits of agreement (which are still below the minimum specified resolution of the PX-26).

2) End-to-End System Specification—Beginning with the sensor's specified accuracy of 0.7 cm H_2O, we sought to filter and acquire data with at least this resolution. With the gain and filtering chosen, our circuit in fact acquires data with 0.18 cm H_2O/LSB, below a "reliable" reading of the sensor. In practice, over several hour long test recordings, the sensor's reading remained fixed, indicating that the true resolution of the system was somewhere between 0.18 cm H_2O and 0.7 cm H_2O. When recordings were extended to days long, 1 LSB change was observed corresponding to the night/day temperature change in the room overnight. In the maternal environment, with the body temperature tightly regulated, we can claim < 1 LSB temperature drift and 0.18 cm H_2O maximum resolution. Full specifications and comparison to the sensor specifications are listed in Table I.

III. *In Vivo* Pilot Experiment

Based on the prototyping detailed above, we created two working implants. One is shown in Fig. 6, with subsequent implantation shown in Fig. 8. The surgical procedure, which we used to implant the device in seven ewes, and data analysis are beyond the scope of this manuscript, but a brief summary follows.

The system was implanted in a 110-day gestational age sheep fetus. Under IACUC approval, ketamine and diazepam were used to initiate ewe anesthesia, followed by maintenance with isoflurane. A midline laparotomy was performed on the pregnant ewe. The uterus was externalized and viable fetus confirmed. An 8 cm hysterotomy was performed in addition to two small 1 cm incisions lateral to the hysterotomy. Two layers of purse string suture were placed around each small incision. Each of the reference and measurement tubes were passed through one of the small incisions, and a Rummel Tourniquet placed to prevent amniotic fluid leak.

The lamb's head was externalized through the hysterotomy and tracheotomy performed. The measurement tube was inserted into the trachea, and secured to the skin using 3.0 prolene sutures. The reference tube was affixed to the fetal skin as close as possible to the tip of the measurement tube. The second measurement tube was placed in the oropharynx, with the reference tube similarly attached outside the mouth. At this point, the purse string sutures were secured and hysterotomy closed with 2.0 maxon suture.

Data were successfully recovered from the device and no errors in recording were noted. Fig. 7 shows example tracings. The top panel, in addition to demonstrating the wide dynamic range of the system, shows widely positive and negative pressure swings that in fact increase beyond the dynamic range. In designing the system, we chose this range based upon previously recorded pressure tracings that relied on catheters open to the atmosphere as mentioned earlier—we believe this is the first fetal pressure recording taken with a fully closed, fully implanted system. It is likely that these are the true pressures seen by the developing lung cells. Future *in vitro* and *in vivo* studies of lung tissue might incorporate the knowledge of a high dynamic stress range in determining the biological pathways responsible for lung growth.

Fig. 7, bottom panel, highlights the high time resolution of the system. The fluctuations here are likely not noise because they were entirely absent during our benchtop test recordings. They are also likely not motion artifact, since our surgical technique ties both pressure and reference tube at very close proximity, so motion (and subsequent hydrostatic pressure change) experienced by one port of the differential pressure sensor would also be experienced by the other port. We believe these fluctuations to be the pressure generated either by diaphragmatic or abdominal muscle contractions. Further classification of these fluctuations could lead to different approaches in *in vitro* study of lung cells, such as subjecting the cell substrate to higher frequency vibrations.

IV. Conclusion

We have demonstrated an *in utero* data logging system capable of measuring low-pressure fluctuations in the fetal pulmonary tree of a lamb. Unlike previous systems, our system has zero exteriorized components. Careful analog circuit design and efficient power management of an SD card was demonstrated, achieving battery life of over 21 days. Initial analysis of data obtained from this system shows greater pressure fluctuations and higher bandwidth events than initially observed in the literature.

Acknowledgment

The authors would like to thank Dr. J. Clements at the University of California, San Francisco, for his invaluable advice and experience with fetal lung physiology, Dr. M. Harrison for his expertise in and creation of the field of fetal surgery, and Dr. O. T. Inan for his circuit design experience.

This work was supported by National Institutes of Health (NIH) Small Business Innovation Research under Grant 1R41HL110466-01, and the Food and Drug Administration through the Pediatric Device Consortium under Grant 2P50FD003793-03. The work of M. Etemadi was supported by the Medical Scientist Training Program grant through the National Institutes of Health. The work of S. C. Schecter was supported by the NIH T32 Training Grant GM008258-23.

Biography

Mozziyar Etemadi (S'07) received the B.S. and M.S. degrees in electrical engineering from Stanford University, Stanford, CA, in 2008 and June 2009, respectively., He is currently working toward the M.D. and Ph.D. degrees in bioengineering at the University of California, San Francisco.

He is currently in the Medical Scientist Training Program at the University of California, San Francisco. His current research interests include translational biomedical engineering for in-home monitoring of disease and biomedical instrumentation for fetal surgery.

Mr. Etemadi was named *Forbes Magazine's* “Top 30 Under 30” in Science in 2012. In 2011, he helped lead of a research team awarded second prize in the Vodafone Americas Wireless Innovation Challenge and the mHealth Alliance Award. While at Stanford University in 2009, he received the Frederick E. Terman Award for Scholastic Achievement in Engineering and also received the Electrical Engineering Fellowship, providing full support for his graduate studies.

J. Alex Heller (S'12) received the B.S. degree in mechanical engineering from the University of Southern California, Los Angeles, in 2008.

He then went on to work for Northrop Grumman, Marine Systems, Sunnyvale, CA. Since 2010, he has worked as an Engineer and Researcher at the University of California, San Francisco, for the Biomedical Microdevices Laboratory and the Pediatric Device Consortium. He is currently enrolled in the joint M.S. Bioengineering program between the University of California, Berkeley and the University of California, San Francisco. His current research is focused on medical devices, specifically, on renal replacement therapy and obstetrics-related devices.

Samuel C. Schecter received the B.A. degree in history from the University of Oregon, Eugene, OR, in 1999, and the M.B.B.S. degree from the University of Queensland, Herston, Qld., Australia, in 2006.

He is currently a General Surgery Resident at the University of California, San Francisco (UCSF) East Bay Surgery Program, and a Research Fellow in the UCSF Division of Pediatric Surgery/Fetal Treatment Center. His research interests include developing in utero therapy for congenital diaphragmatic hernia (CDH), the mechanobiology of the developing lung, and fetal therapy for complicated twin gestation.

Dr. Schecter received first prize in the resident paper competition of the Bay Area Society of Thoracic Surgeons for creating a new form of tracheal occlusion for fetal treatment of CDH in 2011.

Eveline H. Shue received the B.A. degree in biology and psychology from Northwestern University, Evanston, IL, in 2004, and the M.D. degree from the University of Pittsburgh, Pittsburgh, PA, in 2008.

She has completed three years of general surgery residency at the University of California, San Francisco, and is currently in her first of two years of research in the Division of Pediatric Surgery. Her current research projects involve maternal administration of phosphodiesterase type 5 inhibitors to prevent pulmonary hypertension in fetuses with congen ital diaphragmatic hernia.

Dr. Shue received the Lucien B. Rubenstein Award from the American Brain Tumor Association for her project “Characterization of the role of plasmalemmal vesicle associated protein 1 (PV-1) in brain tumor angiogenesis” in 2005.

Doug Miniati received the B.A. degree (*cum laude*) in biochemistry from Dartmouth College, Hanover, NH, in 1992, and the M.D. degree from the New York University School of Medicine, New York, in 1996. He completed his general surgical training at Stanford University, Stanford, CA, in 2004, and a fellowship in pediatric surgery at Texas Children's Hospital (TCH), Baylor College of Medicine, Houston, TX, in 2006.

He is currently an Assistant Professor of surgery at the Division of Pediatric Surgery and Fetal Treatment Center, University of California, San Francisco (UCSF). While at Stanford University and TCH, he developed a clinical interest in congenital diaphragmatic hernia, particularly with respect to the development of treatment strategies to improve outcomes. Now at UCSF, he is the Co-Director of the UCSF Multidisciplinary Congenital Diaphragmatic Hernia Clinic, and continues his clinical and basic science research pursuits, focused on the pathophysiology of lung development, growth, and function.

Shuvo Roy (M'96) received the B.S. degree (*magna cum laude*), with general honors for triple majors in physics, mathematics (special honors), and computer science from Mount Union College, Alliance, OH, in 1992. He also received the M.S. degree in electrical engineering and applied physics and the Ph.D. degree in electrical engineering and computer science from Case Western Reserve University, Cleveland, OH, in 1995 and 2001, respectively.

He is currently an Associate Professor in the Department of Bioengineering and Therapeutic Sci ences, a joint department of the Schools of Pharmacy and Medicine at the University of California, San Francisco (UCSF), and Director of the UCSF Biomedical Microdevices Laboratory. He holds the Harry Wm. and Diana V. Hind Distinguished Professorship in Pharmaceutical Sciences II in the UCSF School of Pharmacy. He is also a Founding Member of the UCSF Pediatric Devices Consortium, which has a mission to accelerate the development of innovative devices for childrens health, and a faculty affiliate of the California Institute for Quantitative Biosciences (QB3). From 1998 to 2008, he was the Co-Director of the BioMEMS Laboratory in the Department of Biomedical Engineering at the Cleveland Clinic, Cleveland, OH, where he worked with basic scientists, practicing

clinicians, and biomedical engineers to develop microelectromechanical systems (MEMS) solutions to high-impact medical challenges. While pursuing his doctorate degree, he conducted research in the areas of design, microfabrication, packaging, and performance of MEMS for harsh environments. He also investigated microstructural characteristics and mechanical properties of MEMS materials, developed the requisite microfabrication technologies, and demonstrated operation of the first surface micromachined silicon carbide transducers at high temperatures (up to 950 °C). He has also developed miniaturized microrelays for high-performance electrical switching and ice detection sensors for aerospace applications. He joined UCSF in 2008 to continue the development of biomedical devices including wireless physiological monitoring systems and bioartificial replacement organs, and participate in the training of professional students in the School of Pharmacy as well as graduate students in the UCSF/University of California, Berkeley Joint Graduate Group in Bioengineering. He has contributed to more than 90 technical publications, coauthored three book chapters, been awarded 16 U.S. patents, and given more than 70 invited presentations.

Dr. Roy is an Associate Editor of *Biomedical Microdevices* and Editorial Board Member of *Sensors and Materials*. He is the recipient of a Top 40 under 40 Award by Crains Cleveland Business in 1999 and the Clinical Translation Award at the second Annual BioMEMS and Biomedical Nanotechnology World 2001 meeting. In 2003, he was selected as a recipient of the TR100, which features the worlds 100 Top Young Innovators as selected by *Technology Review*, the Massachusetts Institute of Technology's Magazine of Innovation. In 2004, he was presented with a NASA Group Achievement Award for his work on harsh environment MEMS. In 2005, he was named as a Whos Who in Biotechnology by Crains Cleveland Business. In 2005 and 2007, he was recognized as a Cleveland Clinic Innovator. In 2009, he was nominated for the Biotechnology Industry Organizations Biotech Humanitarian Award, which is given in recognition of an individual who has used biotechnology to unlock its potential to improve the earth.

References

1. Kitterman JA. The effects of mechanical forces on fetal lung growth. Clin. Perinatol. 1996; 23(4): 727–740. [PubMed: 8982567]
2. Liggins GC. Growth of the fetal lung. J. Develop. Physiol. 1984; 6(3):237–248.
3. Harding R, Hooper SB. Regulation of lung expansion and lung growth before birth. J. Appl. Physiol. 1996; 81(1):209–224. [PubMed: 8828667]
4. Scarpelli EM, Condorelli S, Cosmi EV. Lamb fetal pulmonary fluid. I. Validation and significance of method for determination of volume and volume change. Pediatr. Res. 1975; 9(4):190–195. [PubMed: 1096061]
5. Jansen AH, Chernick V. Fetal breathing and development of control of breathing. J. Appl. Physiol. 1991; 70(4):1431–1446. [PubMed: 2055820]
6. Dawes GS, Fox HE, Leduc BM, Liggins GC, Richards RT. Respiratory movements and rapid eye movement sleep in the foetal lamb. J. Physiol. 1972; 220(1):119–143. [PubMed: 4333826]
7. Meindl JD, Ford AJ. Implantable Telemetry in Biomedical Research. IEEE Tran. Biomed. Eng. Dec; 1984 BME-31(12):817–823.
8. Hermans B, Lewi L, Jani J, Buck F. d. Deprest J, Puers R. Feasibility of in utero telemetric fetal ECG monitoring in a lamb model. Fetal Diagnosis Ther. 2008; 24(2):81–85.

9. Tallaj JA, Singla I, Bourge RC. Implantable hemodynamic monitors. Cardiol. Clin. 2011; 29(2): 289–299. [PubMed: 21459250]

10. Jiang H, Lan D, Goldman K, Etemadi M, Shahnasser H, Roy S. The responsivity of a miniaturized passive implantable wireless pressure sensor. Proc. IEEE Top. Conf. Biomed. Wireless Technol., Netw., Sensing, Syst. 2011:11–14.

11. Woakes AJ, Butler PJ, Bevan RM. Implantable data logging system for heart rate and body temperature: Its application to the estimation of field metabolic rates in Antarctic predators. Med. Biol. Eng. Comput. 1995; 33(2):145–151. [PubMed: 7643651]

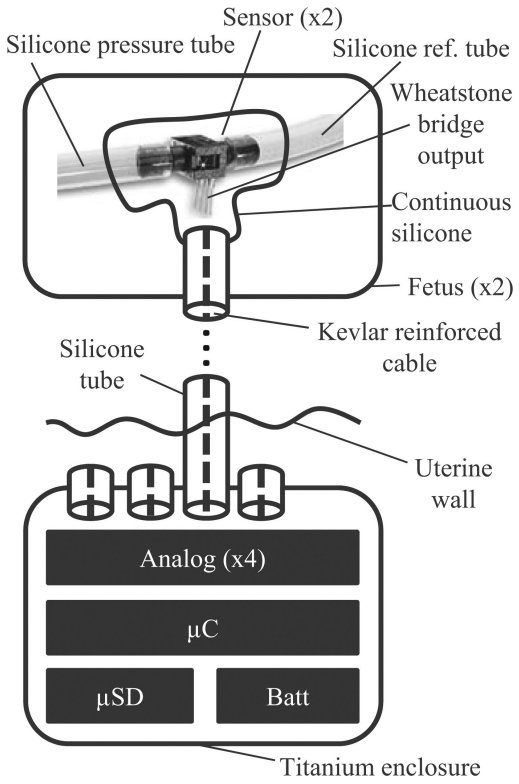

Fig. 1.

Block diagram. For each fetus (typically twins), two pressure transducers are implanted. One measures tracheal pressure, and the other oropharyngeal pressure, both relative to amniotic pressure. The sensors from all the fetuses are connected to one PCB, enclosed in a titanium enclosure implanted in the ewe's abdominal cavity. This PCB contains analog amplification circuitry, A/D conversion, and a microSD card for storage.

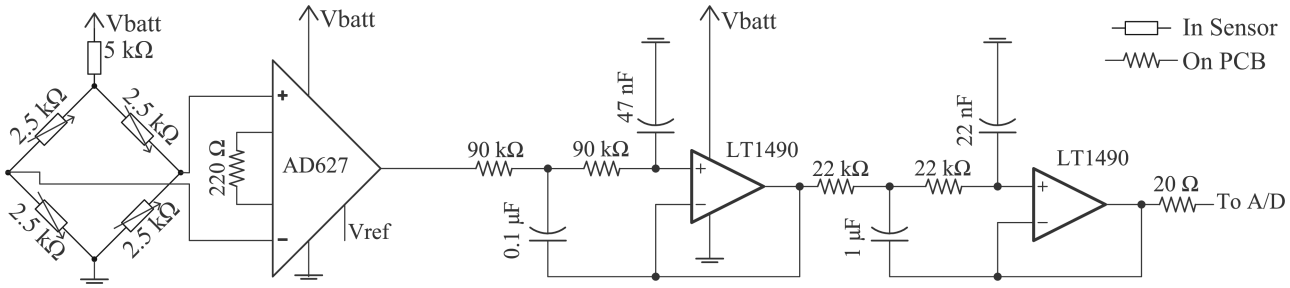

Fig. 2.

Analog Circuit. A commercially available instrumentation amplifier front end amplifies the signal from the strain gauges, which is driven by the dc power supply. To reduce aliasing artifacts, the signal is passed through a fourth-order, 50 Hz cutoff (−3 dB) Sallen–Key low-pass filter prior to sampling. The resulting attenuation at the Nyquist frequency is 44 dB. After the filter, the signal is converted to digital ratiometrically against the same dc power supply voltage. Vref indicates Op-Amp buffered mid-supply voltage. Decoupling capacitors not drawn.

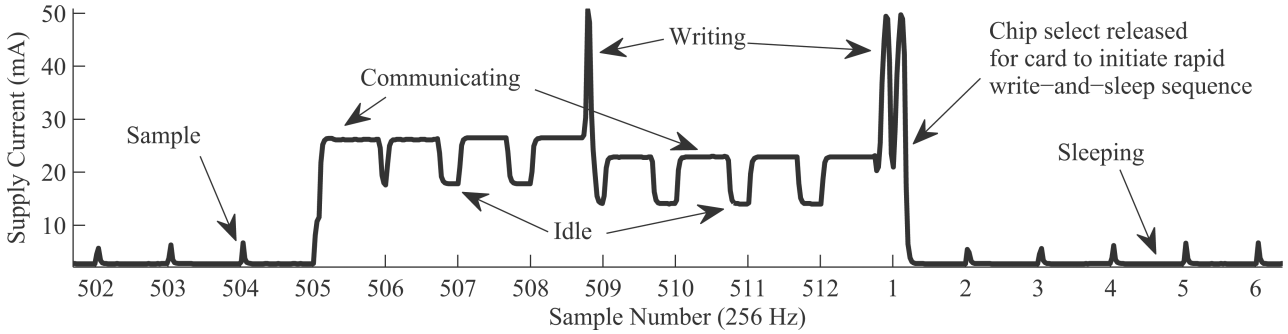

Fig. 3.

Timing diagram. Actual supply current of device measured on high-frequency digital multimeter. Every 512 samples, data are written to the SD card. Between these write cycles, card is forced to lowest power possible state by releasing card's chip select line. This allows for semideterministic behavior, ideal for inexpensive storage in a real-time data logging application.

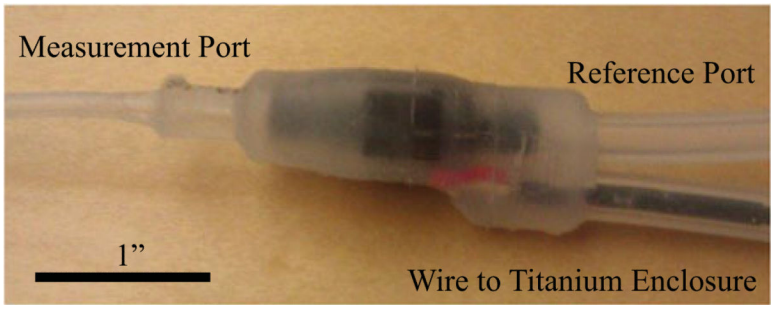

Fig. 4.
One-piece silicone sensor module.

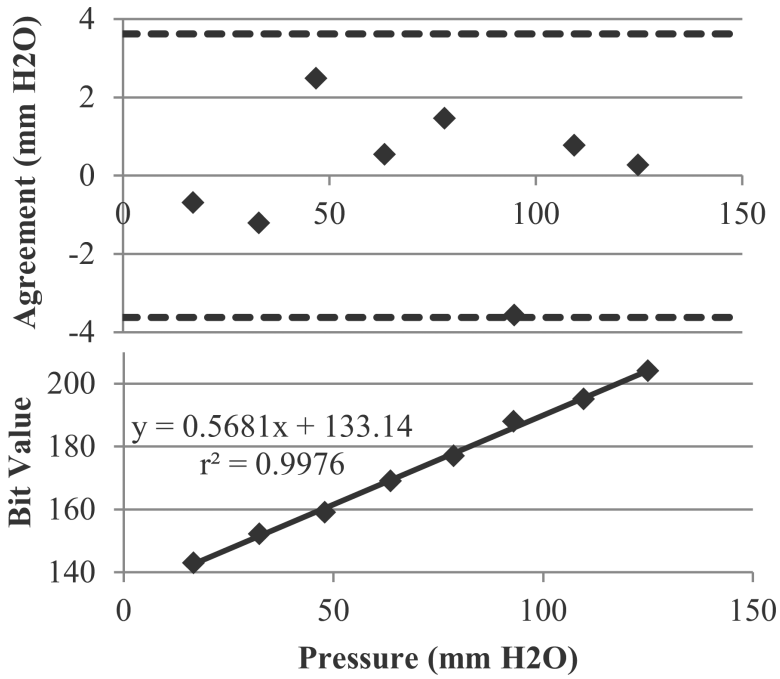

Fig. 5.
Correlation plot and Bland Altman analysis for the end-to-end-system.

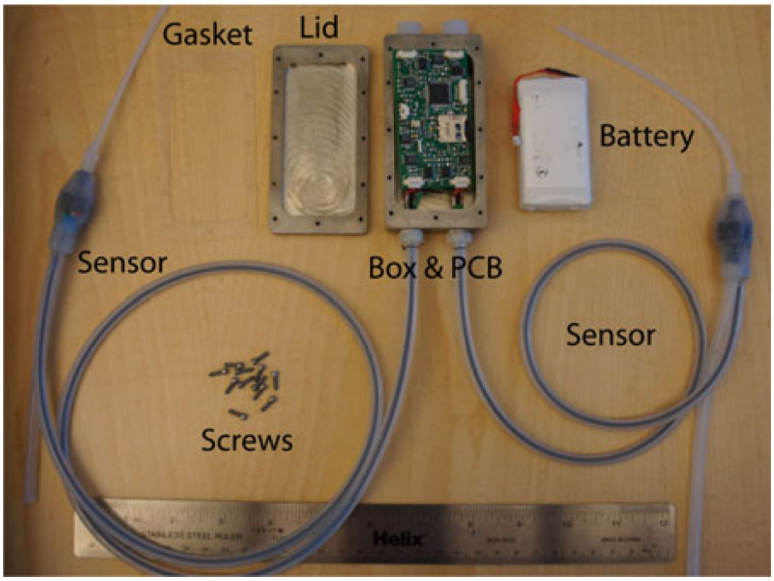

Fig. 6.

Entire implanted system, consisting of titanium enclosure, gasket, PCB, 3-Ah battery, titanium screws, and sensors. With the battery placed beneath the PCB and the gasket and lid in place, the entire enclosure measures 3.8″ × 2″ × 1″.

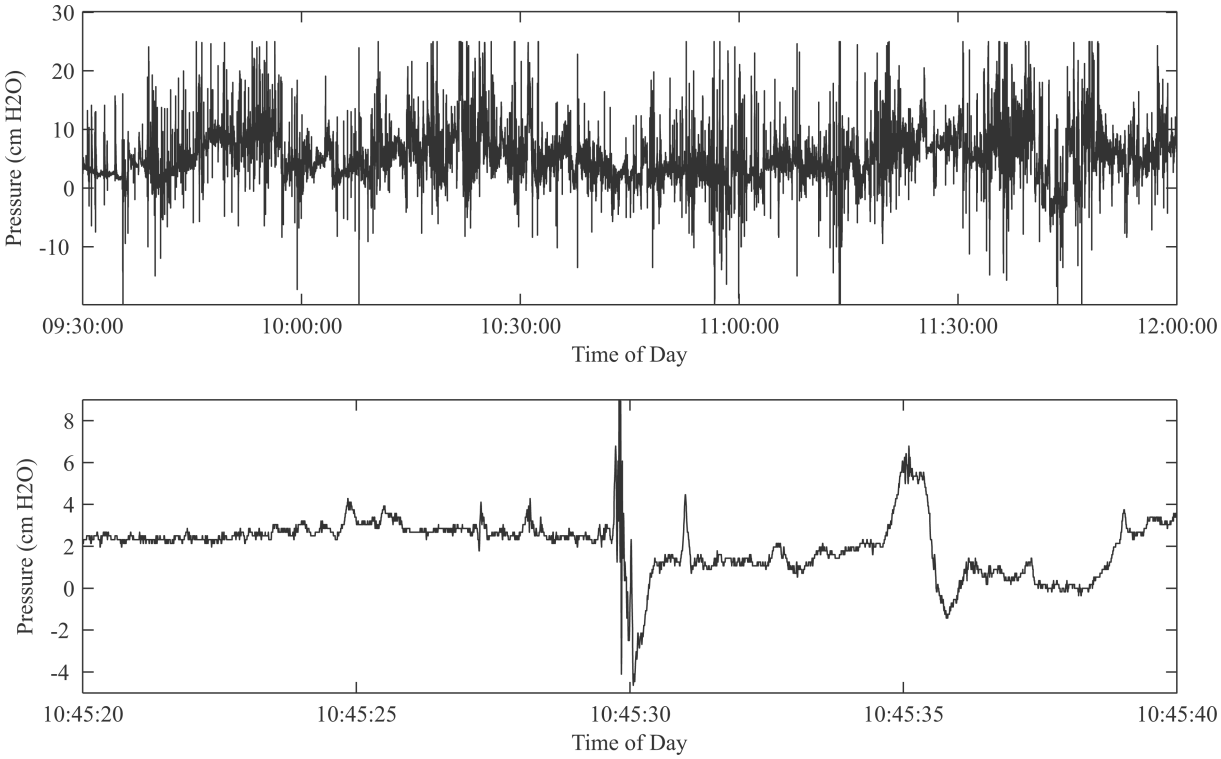

Fig. 7.

(Top) Zoomed-out view of data from live fetus to demonstrate dynamic range and bandwidth of readings over time. Contrary to the literature, both positive and negative swings, and relative nonquiescence are noted. (Bottom) Zoomed-in view of trace demonstrating high-frequency events.

Fig. 8.

Two sensors implanted in a fetal lamb (titanium enclosure not shown). Sensor on the right will measure the tracheal pressure, with the distal end of the measurement tube (not visible) already in the trachea juxtaposed to the visible reference tube. Left sensor's measurement tube is being positioned inside the fetal mouth.

TABLE I

Sensor Specifications Compared to Final System

	PX-26 Spec	End-to-end System
Excitation	0-16 VDC	3.4-4 VDC
Output	1.67 mV/cm H_2O/V[1]	0.18 cm H_2O/LSB
Range	±70 cm H_2O	±20 cm H_2O
Accuracy	0.7 cm H_2O	0.18 cm H_2O
Temp Variability	1mV + 1% Rdg	1 LSB

[1]Units are in millivolts per centimeter of water, per volt of excitation on the bridge. Our system used an excitation voltage that varied based on battery life, anywhere from 3.4 to 4V.